The International Journal of Biochemistry & Cell Biology 45 (2013) 2553–2562

Contents lists available at ScienceDirect

The International Journal of Biochemistry & Cell Biology

journal homepage: www.elsevier.com/locate/biocel

# Lysosomal and mitochondrial permeabilization mediates zinc(II) cationic phthalocyanine phototoxicity

Julieta Marino[a], María C. García Vior[b], Verónica A. Furmento[a], Viviana C. Blank[a], Josefina Awruch[b], Leonor P. Roguin[a,*]

[a] Instituto de Química y Fisicoquímica Biológicas (UBA-CONICET), Facultad de Farmacia y Bioquímica, Junín 956, C1113AAD Buenos Aires, Argentina
[b] Departamento de Química Orgánica, Facultad de Farmacia y Bioquímica, Universidad de Buenos Aires, Junín 956, C1113AAD Buenos Aires, Argentina

ARTICLE INFO

*Article history:*
Received 15 May 2013
Received in revised form 7 August 2013
Accepted 16 August 2013
Available online 28 August 2013

*Keywords:*
Photodynamic therapy
Phthalocyanine
Apoptosis
Lysosomal proteases
Bcl-2 family proteins

ABSTRACT

In order to find a novel photosensitizer to be used in photodynamic therapy for cancer treatment, we have previously showed that the cationic zinc(II) phthalocyanine named Pc13, the sulfur-linked dye 2,9(10),16(17),23(24)-tetrakis[(2-trimethylammonium) ethylsulfanyl]phthalocyaninatozinc(II) tetraiodide, exerts a selective phototoxic effect on human nasopharynx KB carcinoma cells and induces an apoptotic response characterized by an increase in the activity of caspase-3. Since the activation of an apoptotic pathway by chemotherapeutic agents contributes to the elimination of malignant cells, in this study we investigated the molecular mechanisms underlying the antitumor action of Pc13. We found that after light exposure, Pc13 induced the production of reactive oxygen species (ROS), which are mediating the resultant cytotoxic action on KB cells. ROS led to an early permeabilization of lysosomal membranes as demonstrated by the reduction of lysosome fluorescence with acridine orange and the release of lysosomal proteases to cytosol. Treatment with antioxidants inhibited ROS generation, preserved the integrity of lysosomal membrane and increased cell proliferation in a concentration-dependent manner. Lysosome disruption was followed by mitochondrial depolarization, cytosolic release of cytochrome C and caspases activation. Although no change in the total amount of Bax was observed, the translocation of Bax from cytosol to mitochondria, the cleavage of the pro-apoptotic protein Bid, together with the decrease of the anti-apoptotic proteins Bcl-$X_L$ and Bcl-2 indicated the involvement of Bcl-2 family proteins in the induction of the mitochondrial pathway. It was also demonstrated that cathepsin D, but not caspase-8, contributed to Bid cleavage. In conclusion, Pc13-induced cell photodamage is triggered by ROS generation and activation of the mitochondrial apoptotic pathway through the release of lysosomal proteases. In addition, our results also indicated that Pc13 induced a caspase-dependent apoptotic response, being activation of caspase-8, -9 and -3 the result of a post-mitochondrial event.



## 1. Introduction

Photodynamic therapy (PDT) is an emerging method of cancer treatment based on the combination of visible light, a non-toxic photosensitizer and molecular oxygen (Henderson and Dougherty, 1992; Sharman et al., 1999; Allison et al., 2010). Suitable light excitation of the sensitizer preferentially localized within the neoplastic cells results in the induction of an oxidative damage by production of cytotoxic reactive oxygen species (ROS). The formation of ROS triggers the biochemical and molecular events that finally lead to the destruction of cancer cells (Henderson and Dougherty, 1992; Sharman et al., 1999; Allison et al., 2010). Phthalocyanines (Pcs) are a new generation of photosensitizers which possess a strong light absorption at approximately 670 nm, a region where light penetration into tissues is optimal. Consequently, phthalocyanines have been considered as appropriate candidates for PDT applications (Taquet et al., 2007; Calzavara-Pinton et al., 2007). In this sense, different studies have assessed the photodynamic efficiency of various zinc (Margaron et al., 1996), aluminum (Paquette et al., 1991; Boyle et al., 1992; Allen et al., 2002), and silicon phthalocyanines (Colussi et al., 1999) as antitumor agents. In particular, the silicon phthalocyanine named Pc4 induced an apoptotic response after PDT and has been evaluated in a phase I clinical trial for the treatment of cutaneous malignancies, such as cutaneous T-cell lymphoma (Miller et al., 2007).

*Abbreviations:* Ac-DEVD-AMC, Ac-Asp-Glu-Val-Asp 7-amino-4-methylcoumarin; Ac-LEHD-AMC, Ac-Leu-Glu-His-Asp 7-amino-4-methylcoumarin; DCFH-DA, 2′,7′-dichlorfluorescein diacetate; $DiOC_6(3)$, 3,3′-dihexyloxacarbocyanine iodide; PDT, photodynamic therapy; Pc, phthalocyanine; PI, propidium iodide; ROS, reactive oxygen species; Z-IETD-AFC, Z-Ile-Glu-Thr-Asp 7-amido-4-trifluoromethyl coumarin; Z-VAD-FMK, Z-Val-Ala-Asp(O-Me) fluoromethylketone.

* Corresponding author. Tel.: +54 11 4964 8290; fax: +54 11 4962 5457.
*E-mail addresses:* rvroguin@qb.ffyb.uba.ar, rvroguin@gmail.com (L.P. Roguin).

1357-2725/$ – see front matter © 2013 Elsevier Ltd. All rights reserved.
http://dx.doi.org/10.1016/j.biocel.2013.08.012

Although several Pcs can be effective photosensitizers, many of them lose their phototoxic ability in aqueous solution due to the formation of inactive aggregates (Li et al., 2008). In order to improve the amphiphilic properties, we have previously synthesized a group of isosteric water-soluble cationic zinc(II) phthalocyanines and demonstrated that one of them, the sulfur-linked phthalocyanine named 2,9(10),16(17),23(24)-tetrakis[(2-trimethylammonium) ethylsulfanyl]phthalocyaninatozinc(II) tetraiodide (Pc13), was the most active sensitizer leading to human nasopharynx KB carcinoma cell death (Marino et al., 2010). This compound, localized preferentially within lysosomes, induced an apoptotic response characterized by chromatin condensation, an increase in the activity of caspase-3 and the cleavage of the caspase-3 substrate poly-ADP-ribose-polymerase (PARP) (Marino et al., 2010).

The balance between apoptotic and survival signals is implicated in the physiological fate of a cell. However, whereas an apoptotic response should be effective for the elimination of tumor cells, it could also be responsible for tissue damage. In this respect, an excessive cell death has been found in human diseases characterized by cellular organelle dysfunction and activation of oxidative stress pathways produced by the accumulation of misfolded proteins (Lawless et al., 2008). In order to evaluate the molecular mechanisms underlying the apoptotic response triggered by Pc13, we inquired whether this lysosome-targeted photosensitizer could induce a lysosomal damage related to the activation of a mitochondrial apoptotic pathway. In this sense, it has been reported that those photosensitizers mainly accumulated in lysosomes are able to produce not only the disruption of these organelles upon irradiation, but also the permeabilization of mitochondria membrane (Reiners et al., 2002; Chiu et al., 2010; Liu et al., 2011). Based on these findings, it has been shown that the release of lysosomal proteases into the cytosol could represent an initial event that contributes to mitochondrial injury and the execution of an apoptotic program of cell death (Guicciardi et al., 2004; Chwieralski et al., 2006; Boya and Kroemer, 2008; Johansson et al., 2010).

In this study, we first showed that cell death induced by Pc13 was mediated by the generation of ROS. We then demonstrated that, after photodynamic treatment, the oxidative response elicited the early permeabilization of lysosomal membranes and the resulting release of lysosomal proteases, such as cathepsin D. Consequently, a change in some pro-apoptotic Bcl-2 family proteins was observed, followed by the loss of mitochondrial membrane potential ($\Delta\Psi_m$), the liberation of cytochrome C and the activation of caspases, which finally lead to cell death.

## 2. Materials and methods

### 2.1. Chemicals

Synthesis and purification of the sulfur-linked cationic 2,9(10),16(17),23(24)-tetrakis[(2-trimethylammonium)ethylsulfanyl]phthalocyaninatozinc(II) tetraiodide, named Pc13, has been previously described (Marino et al., 2010). Pepstatin A, monoclonal antibodies against cathepsin D, Bax, and polyclonal anti-Bid, Bcl-2 and Bcl-$X_L$ antibodies were obtained from Santa Cruz Biotechnology (Santa Cruz, CA). Mouse monoclonal antibody directed against cytochrome C was from BD Biosciences Pharmingen (San Diego, CA). Polyclonal antibodies against caspase-3, cleaved caspase-3, caspase-8, and monoclonal anti-caspase-9 antibody were purchased from Cell Signaling Technology (Danvers, MA). The secondary antibody anti-mouse IgG conjugated with Alexa Fluor and the fluorescent dye MitoTracker Green FM were obtained from Invitrogen (San Diego, CA). Caspase substrates Ac-DEVD-AMC (caspase-3), Z-IETD-AFC (caspase-8) and Ac-LEHD-AMC (caspase-9) were obtained from Calbiochem (Billerica, MA). Acridine orange, ascorbic acid, leupeptin, the probe 2′,7′-dichlorfluorescein diacetate (DCFH-DA), the antioxidant 6-hydroxy-2,5,7,8-tetramethylchroman-2-carboxylic acid (trolox) and the fluorescent dye 3,3′-dihexyloxacarbocyanine iodide ($DiOC_6(3)$) were from Sigma Chemical (St. Louis, MO). Caspase-8 inhibitor (Z-IETD-FMK) and the pan inhibitor Z-VAD-FMK were from Santa Cruz Biotechnology (Santa Cruz, CA).

### 2.2. Cells and culture conditions

Human nasopharynx carcinoma KB cells (ATCC CCL-17) were maintained in Minimum Essential Medium (MEM, Gibco BRL) containing 10% (v/v) fetal bovine serum (FBS, Gibco BRL), 2 mM L-glutamine, 50 U/mL penicillin, 50 mg/mL streptomycin, 1 mM sodium pyruvate and 4 mM sodium bicarbonate, in a humidified atmosphere of 5% $CO_2$ at 37 °C.

### 2.3. Photodynamic treatment

KB cells ($5 \times 10^3$/well) were grown in MEM supplemented with 10% FBS and incubated overnight at 37 °C until 70–80% of confluence. A 5 μM solution of phthalocyanine 13 was added in culture medium containing 4% FBS. After incubating cells for 24 h, the compound was removed and then complete fresh culture medium was added and cells were exposed to a light dose required to obtain approximately 50% of cell growth (1.4 J $cm^{-2}$) with a 150 W halogen lamp equipped with a 10 mm water-filter to maintain cells cool and attenuate IR radiation. In addition, a cut-off filter was employed to bar wavelengths shorter than 630 nm. In parallel, cells irradiated in the absence of Pc13 were used as control. In some experiments, cells were pre-incubated for 1 h before irradiation with different concentrations of antioxidants (trolox or ascorbic acid), the caspase pan inhibitor Z-VAD-FMK, pepstatin A or leupeptin. After light exposure, cells were incubated for an additional 24 h period and cell number was evaluated by colorimetric determination of hexosaminidase levels, an ubiquitous lysosomal enzyme (Landegren, 1984). Briefly, cells were washed twice with phosphate-buffered saline (PBS) and then incubated at 37 °C with 60 μL of 3.25 mM p-nitrophenol-N-acetyl-β-D-glucosaminide dissolved in 50 mM citrate buffer, pH 5, 0.25% Triton X-100. After 45 min, the color reaction was developed and enzyme activity was blocked by adding 90 μL of 50 mM glycine buffer, pH 10.4, containing 5 mM EDTA. Absorbance values were measured at 405 nm in a Biotrack II Microplate Reader (GE Healthcare, Piscataway, NY).

### 2.4. Determination of intracellular ROS production

The endogenous ROS content was evaluated from the oxidation of the probe 2′,7′-dichlorfluorescein diacetate (DCFH-DA). After diffusing into cells, DCFH-DA is first deacetylated by esterases and then is oxidized by hydrogen peroxide or peroxides to produce the fluorescent 2′,7′-dichlorfluorescein (DCF). KB cells were plated at a density of $6 \times 10^4$ cells/well in 24-well microplates and incubated overnight at 37 °C until 70–80% of confluence. Then, the culture medium was replaced by MEM containing 4% FBS and 5 μM of Pc13. After 24 h, the compound was removed, cells were pre-incubated 1 h at 37 °C in the absence or presence of 5 mM trolox or 10 mM ascorbic acid, and irradiated with a light dose of 2.8 J $cm^{-2}$. Cells were then washed with PBS and treated in the presence of 10 μM DCFH-DA at 37 °C for 20 min. Non-incorporated probe was eliminated by washing the cells twice with PBS. Cells were solubilized with Triton X-100 (0.1%, v/v) in PBS, and the fluorescence of DCF was detected in a PerkinElmer LS55 Fluorometer (PerkinElmer Ltd., Beaconsfield, UK) using 488 nm excitation and 530 nm emission wavelengths. After 10 min of incubation with a final concentration of 50 μM propidium iodide (PI), DNA content was estimated from the fluorescence intensity of DNA-PI complex at excitation

and emission wavelengths of 538 and 590 nm, respectively. Results were expressed as the ratio between DCF and PI fluorescence. Alternatively, cells were grown in coverslips to examine the green fluorescence of DCF with a fluorescence Olympus BX50 microscope with the corresponding filter, at 470–490 nm excitation and 515 nm emission wavelengths.

Alternatively, cells were solubilized with Triton X-100 (0.1%, v/v) in PBS, and the fluorescence of DCF was detected in a PerkinElmer LS55 Fluorometer (PerkinElmer Ltd., Beaconsfield, UK) using 488 nm excitation and 530 nm emission wavelengths. After 10 min of incubation with a final concentration of 50 μM propidium iodide (PI), DNA content was estimated from the fluorescence intensity of DNA-PI complex at excitation and emission wavelengths of 538 and 590 nm, respectively. Results were expressed as the ratio between DCF and PI fluorescence.

### 2.5. Western blot assays

KB cells were incubated during 24 h with a 5 μM solution of Pc13, then washed with PBS and exposed to a light dose of 2.8 J cm$^{-2}$. In some experiments, cells were pre-incubated for 1 h with 5 mM trolox or 20 μM caspase-8 inhibitor (Z-IETD-FMK), or for 24 h with 100 μM pepstain A. After irradiation, suspensions containing $1 \times 10^6$ cells were immediately lysed for 30 min at 4 °C in 10 μL of lysis buffer (0.5% Triton X-100, 1 μg/mL aprotinin, 1 μg/mL trypsin inhibitor, 1 μg/mL leupeptin, 10 mM $Na_4P_2O_7$, 10 mM NaF, 1 mM $Na_3VO_4$, 1 mM EDTA, 1 mM PMSF, 150 mM NaCl, 50 mM Tris, pH 7.4). Alternatively, irradiated cells were incubated for different time-periods at 37 °C and then cell lysates were prepared. Clear supernatants were centrifuged at 17,000 × *g* for 10 min at 4 °C and protein concentration was determined using Bradford reagent. Aliquots containing 50 μg of protein were resuspended in 0.063 M Tris/HCl, pH 6.8, 2% SDS, 10% glycerol, 0.05% bromophenol blue, 5% 2-ME, submitted to SDS-PAGE and then transferred onto nitrocellulose membranes (GE Healthcare, Piscataway, NY) for 1 h at 100 V in 25 mM Tris, 195 mM glycine, 20% methanol, pH 8.2. After blocking with 10 mM Tris, 130 mM NaCl and 0.05% Tween 20, pH 7.4, TBS-T, containing 3% bovine serum albumin (BSA), membranes were treated as the usual western blotting method. The applied secondary antibodies anti-mouse IgG (horseradish peroxidase-conjugated goat IgG) or anti-rabbit IgG (horseradish peroxidase-conjugated goat IgG) were from Santa Cruz Biotechnology, CA, USA. Immunoreactive proteins were visualized using the ECL detection system (Amersham Biosciences, Piscataway, NY) according to the manufacturer's instructions. For quantification of band intensity, Western blots were scanned using a densitometer (Gel Pro Analyzer 4.0). Equal protein loading was confirmed by reprobing membranes either with polyclonal rabbit anti-actin antibody (Sigma–Aldrich, Inc., MO) or monoclonal antibody to alpha tubulin (Abcam, MA).

### 2.6. Subcellular fractionation and immunodetection of cathepsin D and cytochrome C

KB cells were incubated during 24 h with or without 5 μM Pc13, then washed with PBS and exposed to a light dose of 2.8 J cm$^{-2}$. In some experiments, cells were pre-incubated 1 h at 37 °C in the absence or presence of 5 mM trolox. After irradiation, cells were incubated for different time-periods at 37 °C and then, for the detection of cathepsin D or cytochrome C, suspensions containing $2 \times 10^6$ cells were washed twice with sucrose buffer (250 mM sucrose, 20 mM HEPES, pH 7.5, 10 mM KCl, 1.5 mM $MgCl_2$, 1 mM EDTA, 1 mM EGTA, 1 mM DTT, 0.1 mM PMSF, 1 μg/mL aprotinin, 1 μg/mL leupeptin), resuspended in 20 μL of sucrose buffer and incubated on

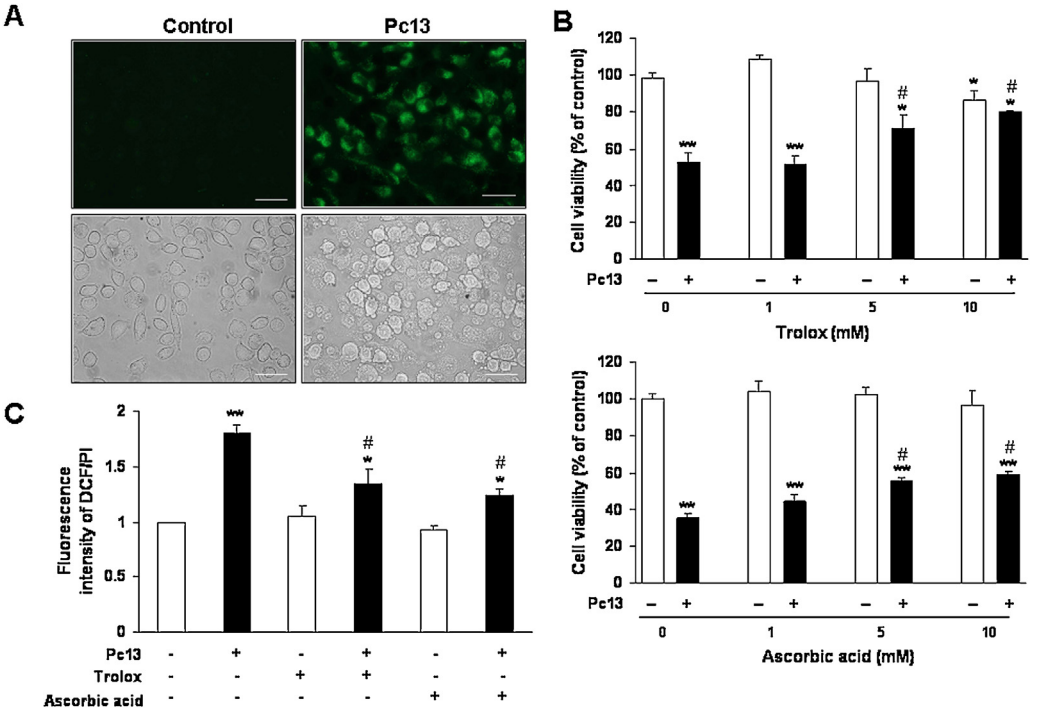


**Fig. 1.** ROS production after irradiation of Pc13-treated cells. (A) KB cells plated on coverslips were incubated with 5 μM Pc13 and then irradiated with a light dose of 2.8 J cm$^{-2}$. ROS formation immediately after irradiation was determined with 10 μM DCFH-DA and detected with a fluorescence microscope (upper panel). Cell morphology was also examined (lower panel). Magnification 400×, scale bar 50 μm. (B) Cell growth after photodynamic treatment with Pc13 was determined in the absence or presence of different concentrations of antioxidants by the hexosaminidase method. $^*p < 0.005$, $^{**}p < 0.001$, significantly different from control (absence of Pc13); $^\#p < 0.05$ significantly different from cells treated with Pc13 in the absence of antioxidants. (C) Quantitative evaluation of ROS levels was performed with a fluorometer after irradiation of Pc13-loaded cells incubated in the absence or presence of 5 mM trolox or 10 mM ascorbic acid. DNA content was estimated after incubating with PI. Results, expressed as the ratio between DCF and PI fluorescence, represent the mean ± S.E.M. of three different experiments. $^*p < 0.05$, $^{**}p < 0.005$, significantly different from control (absence of Pc13); $^\#p < 0.05$ significantly different from Pc13-treated cells (without antioxidants).

ice for 15 min. Cells were then homogenized with a Dounce (40 strokes) and centrifuged at 1000 × *g* for 10 min at 4 °C. The resulting supernatant was subjected to 20,000 × *g* for 20 min at 4 °C. Pellets containing membrane fraction (lysosomal/mitochondrial fraction, 5 μg of protein/lane) or supernatants (10 μg of protein/lane) were loaded onto a SDS-PAGE, transferred onto PVDF membranes and revealed with specific antibodies against cathepsin D or cytochrome C. Quantification of band intensities was performed by using a densitometer (Gel Pro Analyzer 4.0). Actin was employed as loading control of cytosolic fraction, whereas Coomassie Blue staining of PVDF membranes was used to control protein load of lysosomal/mitochondrial fraction (Welinder and Ekblad, 2011).

### 2.7. Lysosomal stability assessment

KB cells were grown on coverslips and incubated in the presence or absence of a 5 μM solution of Pc13 for 24 h at 37 °C in the dark. After photodynamic treatment with 2.8 J cm$^{-2}$, cells were stained with acridine orange (5 μM, 30 min, 37 °C) to label lysosomes (Boya et al., 2003) and then examined with a fluorescence Olympus BX50 microscope with the corresponding filter, 470–490 nm excitation and 515 nm emission wavelengths.

### 2.8. Immunocytochemistry

KB cells grown on coverslips were incubated in the presence or absence of 5 μM Pc13 for 24 h at 37 °C in the dark. After removing the compound with PBS, cells were stained with LysoTracker Green (75 nM, 2 h) diluted in the culture medium without FBS. Then, cells were exposed to a light dose of 2.8 J cm$^{-2}$ and fixed for 5 min at room temperature with 4% paraformaldehyde. Coverslips were washed with PBS/0.25% Triton X-100 and then incubated with anti-cathepsin D antibody for 24 h. This antibody was revealed with a secondary antibody conjugated with Alexa Fluor 568. Alternatively, Pc13-treated cells were stained with MitoTracker Green (100 nM, 45 min) diluted in the culture medium without FBS, then irradiated and incubated for 1 h previous to fixation. Coverslips were washed, incubated with anti-Bax antibody for 24 h, and then with a secondary antibody conjugated with Alexa Fluor 568. Fluorescence was then examined with a confocal microscopy Olympus FV 300. Alexa Fluor 568 was excited at 559 nm and its emission was monitored at 675 nm, and lysosomes or mitochondrias were excited at 473 nm and green fluorescence was detected at 545 nm. Hoescht 33258 was employed to stain nuclei (excitation λ 405 nm, emission λ 460 nm).

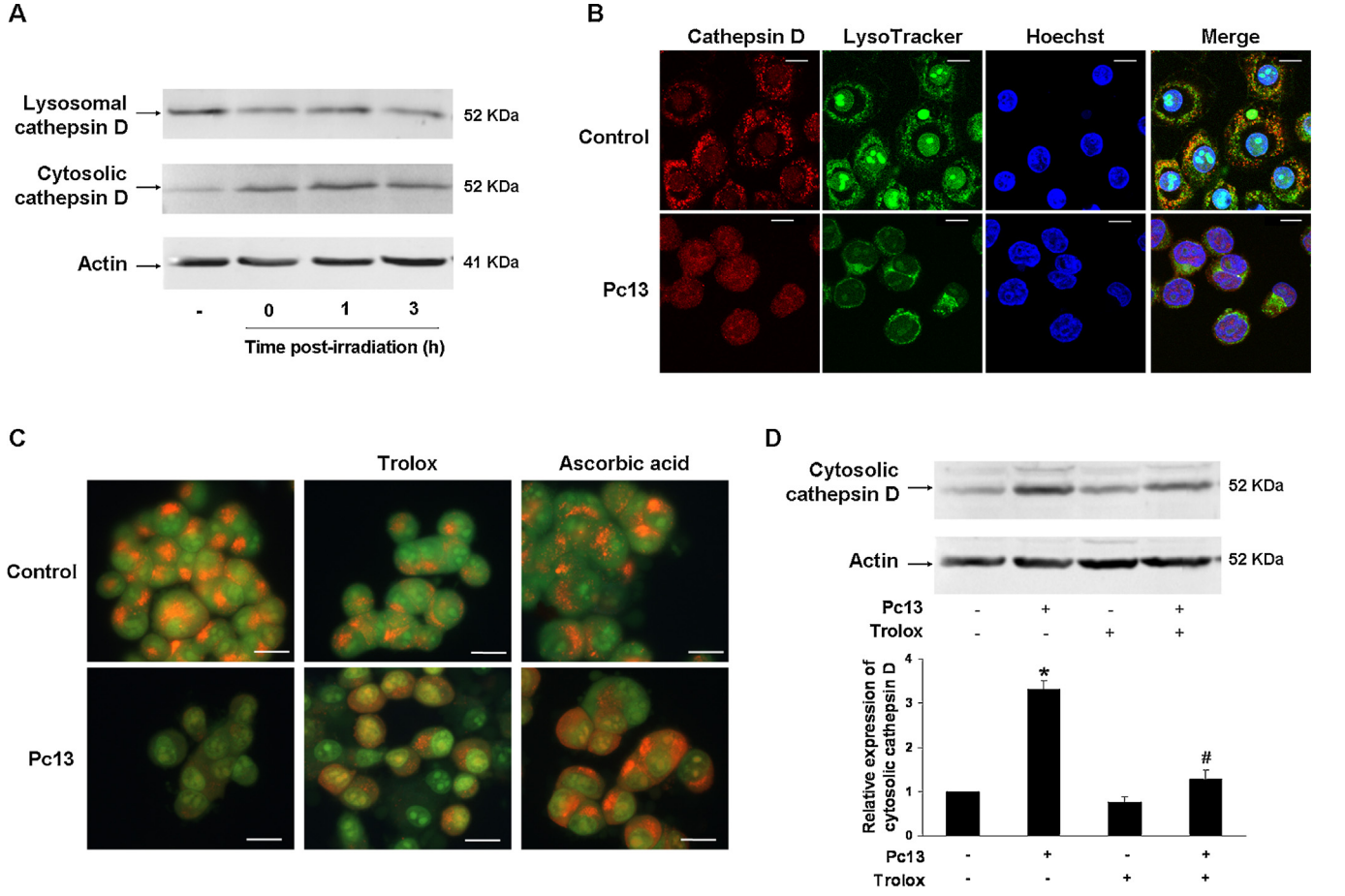


**Fig. 2.** Lysosomal membrane permeabilization induced by photodynamic treatment. (A) KB cells exposed to 5 μM Pc13 were irradiated (time 0 post-irradiation), incubated for 1 or 3 h and submitted to Western blot assays. Cathepsin D was detected both in lysosomal and cytosolic fractions as described in Section 2. Non-treated cells (−) were used as control. (B) KB cells grown on coverslips were incubated in the presence or absence of 5 μM Pc13 in the dark and then stained with LysoTracker Green. After irradiation, cells were fixed, incubated with anti-cathepsin D antibody and revealed with a secondary antibody conjugated with Alexa Fluor 568. Nuclei were stained with Hoescht. Magnification 600×, scale bar 10 μm. (C) Cells plated on coverslips were incubated with or without Pc13 and irradiated in the absence or presence of 5 mM trolox or 10 mM ascorbic acid as described in Section 2. After photodynamic treatment, lysosomes were stained with 5 μM acridine orange and examined in a fluorescence microscope. Magnification 600×, scale bar 20 μm. (D) Pc13-loaded cells were incubated in the absence or presence of 5 mM trolox and after irradiation cytosolic fractions were submitted to Western blot assays. Results from one representative experiment are shown in (A) and (D). Densitometric analyses, expressed as the relationship of cytosolic cathepsin D from Pc13-treated cells with respect to non-treated cells, correspond to mean ± S.E.M. of three different experiments. $^{*}p < 0.001$, significantly different from control (absence of Pc13); $^{\#}p < 0.005$ significantly different from Pc13-treated cells (without trolox).

### 2.9. Evaluation of mitochondrial membrane potential

To measure $\Delta\Psi_m$, KB cells pre-loaded with or without 5 μM Pc13 for 24 h at 37 °C in the dark were treated with a light dose of 2.8 J cm$^{-2}$. After 60 min, cells were incubated with 40 nM of the potential-sensitive cationic lipophilic dye 3, 3′-dihexyloxacarbocyanine iodide ($DiOC_6(3)$) for 30 min at 37 °C. Green fluorescence for $DiOC_6(3)$ was measured by using a FACScan flow cytometer (Becton Dickinson, CA, USA).

### 2.10. Caspase activity assay

After incubating KB cells for 24 h with a 5 μM solution of Pc13, cells were washed and then irradiated with a light dose of 2.8 J cm$^{-2}$ as previously described. Cells were then incubated for different time-periods at 37 °C and $1 \times 10^6$ cells were lysed for 30 min at 4 °C in 50 μL of lysis buffer (10 mM HEPES, pH 7.4, 50 mM NaCl, 2 mM $MgCl_2$, 5 mM EGTA, 1 mM PMSF, 2 μg/mL leupeptin, 2 μg/mL aprotinin) followed by three cycles of rapid freezing and thawing. Cell lysates were centrifuged at 17,000 × *g* for 15 min and total protein concentration was determined using Bradford reagent. Aliquots containing 100 μg of protein were diluted in assay buffer (20 mM HEPES, 132 mM NaCl, 6 mM KCl, 1 mM $MgSO_4$, 1.2 mM $K_2HPO_4$, pH 7.4, 20% glycerol, 5 mM DTT), and incubated at 37 °C for 2 h with 50 μM of the corresponding fluorogenic substrate for caspase-3 (Ac-DEVD-AMC), caspase-8 (Z-IETD-AFC) and caspase-9 (Ac-LEHD-AMC). Cleavage of the substrates was monitored by AMC or AFC release in a SFM25 Konton Fluorometer at 355 or 400 nm excitation and 460 or 505 nm emission wavelengths, respectively. Results were expressed as the change in fluorescence units (per μg of protein) in relation to control (non-treated cells). In some experiments, cells pre-incubated for 24 h with 100 μM pepstatin A were irradiated with a light dose of 1.4 J cm$^{-2}$ and 3 h post-irradiation cell were lysed as described above.

### 2.11. Statistical analysis

The values are expressed as mean ± S.E.M. Statistical analysis of the data was performed by using the Student's *t*-test. $p < 0.05$ denotes a statistically significant difference.

## 3. Results and discussion

### 3.1. Photodynamic treatment with Pc13 induces ROS production in KB cells

It has been previously reported that Pc13 is a photosensitizer potentially useful as a cytotoxic drug for photodynamic therapy (PDT). Although this sulfur-linked cationic aliphatic phthalocyanine showed, in homogeneous solution, a quantum yield of singlet oxygen production ($\Phi_\Delta$) similar to that obtained for the oxygen-linked cationic isosteric phthalocyanine 2,9(10),16(17),23(24)-tetrakis[(2-trimethylammonium)-ethoxy]phthalocyaninatozinc(II) tetraiodide (Pc11), Pc13 but not Pc11 showed an effective phototoxic activity in KB tumor cells (Marino et al., 2010). In addition, no effect on cell proliferation was observed for Pc13 in the dark. In order to demonstrate intracellular ROS generation, KB cells pre-loaded with Pc13 and exposed to a light dose of 2.8 J cm$^{-2}$ were treated with DCFH-DA, a probe which is oxidized by ROS to produce the green fluorescent dye DCF. As shown in Fig. 1A, fluorescence microscopy revealed a marked increase in DCF fluorescence immediately after cell irradiation (time 0 post-irradiation). Since the generation of cytotoxic species would be responsible for triggering the intracellular oxidative damage involved in cell destruction (Henderson and Dougherty, 1992; Sharman et al., 1999; Allison et al., 2010), we then explored the effect of two antioxidants on the growth inhibitory activity induced by Pc13. When KB cells were treated with trolox or ascorbic acid, cell proliferation increased in a concentration-dependent manner, being the maximum effect obtained at final concentrations between 5 and 10 mM of trolox or ascorbic acid (Fig. 1B). It was also showed that both antioxidants partially inhibited the formation of ROS in irradiated Pc13-treated cells (Fig. 1C). Taken together, these results indicate that ROS are mediating the phototoxic effect triggered by Pc13 in KB cells.

### 3.2. Pc13 induces permeabilization of lysosomal membranes

The sequence of molecular events activated after ROS formation, which finally lead to KB cell death, was next examined. It has been reported that cellular photodamage begins in the organelle that retains the photosensitizer (Oleinick et al., 2002; Chiu et al., 2010). Thus, based on our previous results showing that Pc13 is a lysosome-targeted photosensitizer (Marino et al., 2010), we decided to explore whether the phototoxic effect of Pc13 alters lysosomal membranes. When the cytosolic release of the lysosomal enzyme cathepsin D (Hasilik, 1992) was studied at different times after irradiation of Pc13-loaded cells, significant levels of this protease were found at time 0 post-irradiation (Fig. 2A), indicating that lysosomal membrane permeabilization would be an early event in the mechanism of action of Pc13. Consequently, a decrease in the lysosomal amount of cathepsin D was also detected (Fig. 2A). In addition, cathepsin D release was observed immediately after irradiation by confocal microscopy (Fig. 2B). Thus, the

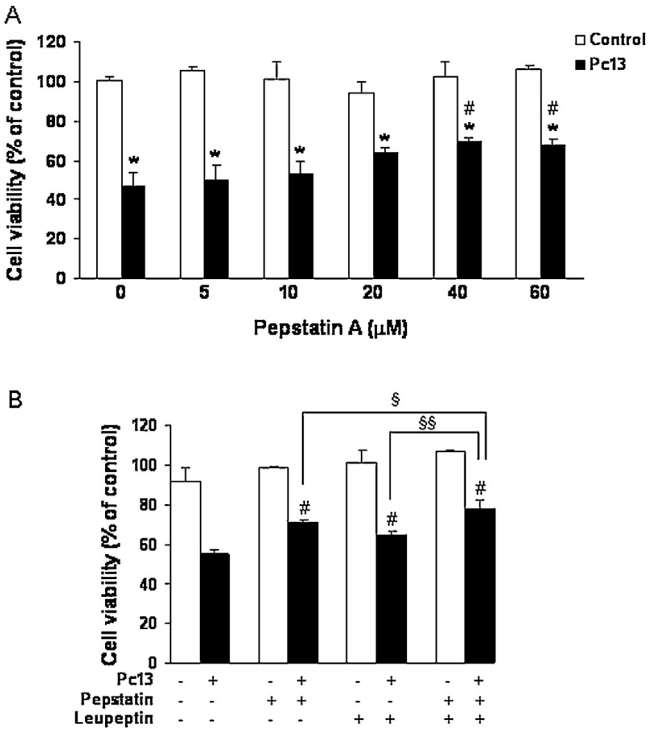


**Fig. 3.** Effect of the inhibition of cathepsins on Pc13-induced cell death. (A) KB cells treated or not with 5 μM Pc13 were pre-incubated 1 h before irradiation with different concentrations of pepstatin A. $^*p < 0.05$, significantly different from control (absence of Pc13); $^\#p < 0.05$ significantly different from cells treated with Pc13 in the absence of pepstatin A. (B) Cells exposed to 5 μM Pc13 were pre-treated 1 h before irradiation with 40 μM pepstatin A, 25 μM leupeptin or with a combination of both inhibitors. $^\#p < 0.01$, significantly different from cells treated with Pc13 in the absence of proteases inhibitors; $^\S p < 0.05$, $^{\S\S} p < 0.01$, significantly different from Pc13-treated cells preincubated with either pepstatin A or leupeptin. Cell growth was determined by the hexosaminidase method.

punctuate pattern of red fluorescence corresponding to cathepsin D co-localized with the green fluorescence of the specific lysosome probe in non-treated cells, whereas irradiated Pc13-loaded cells showed a diffuse cathepsin staining (Fig. 2B). We further studied the effect of antioxidants on Pc13-induced lysosomal membrane permeabilization after staining lysosomes with the fluorescent dye acridine orange. As shown in Fig. 2C, the phototoxic effect of Pc13 led to a marked reduction of orange fluorescence at time 0 post-irradiation. However, when KB cells were incubated in the presence of either trolox or ascorbic acid, the decrease of acridine orange fluorescence was almost undetectable. In accordance with this result, we also showed that expression levels of cytosolic cathepsin D significantly diminished in the presence of trolox, indicating that ROS would be involved in the partial permeabilization of lysosomal

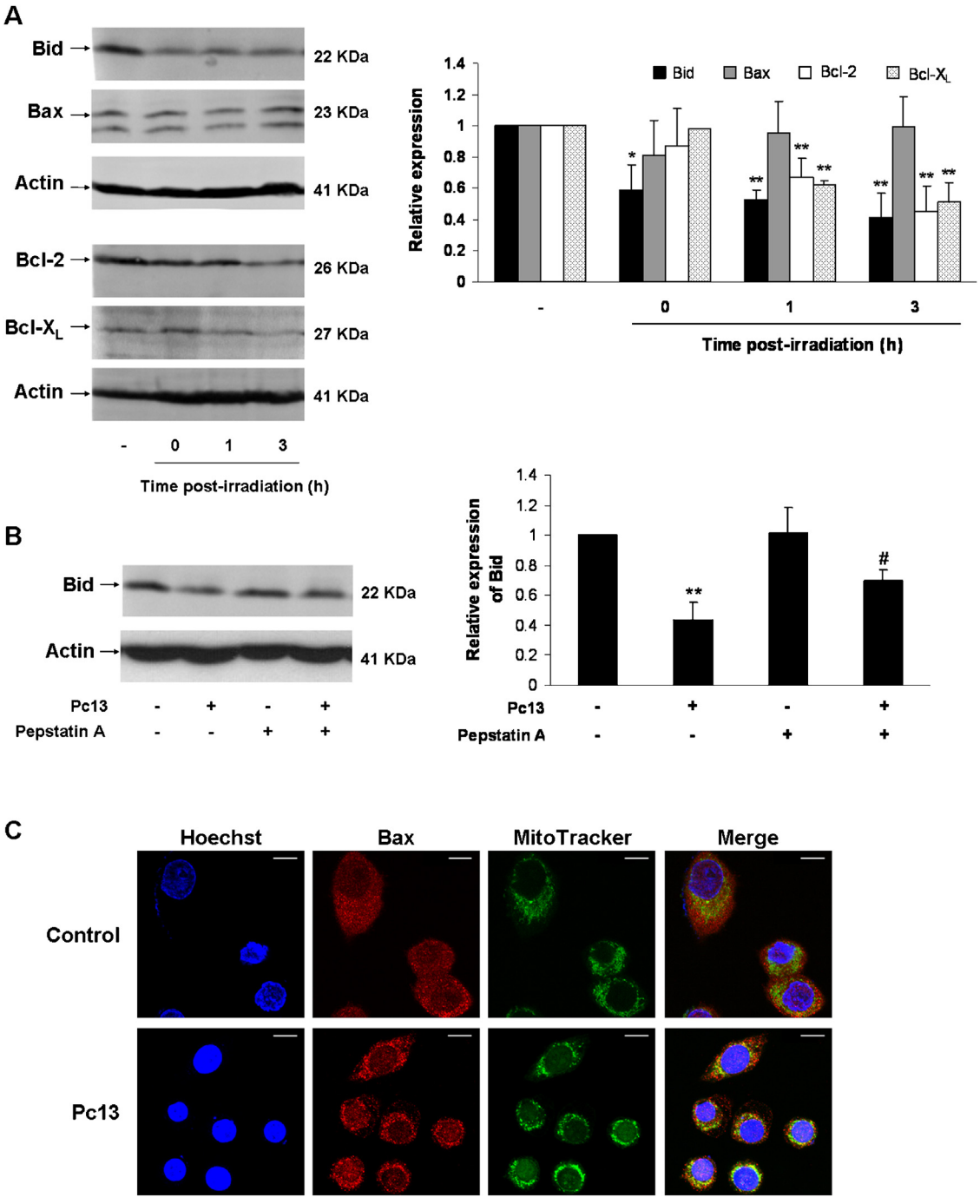


**Fig. 4.** Levels of Bcl-2 family proteins and Bax translocation after photodynamic treatment. (A) Lysates of KB cells exposed to 5 μM Pc13 were irradiated (time 0 post-irradiation), incubated for different times post-irradiation and submitted to Western blot assays. (B) KB cells treated or not with 5 μM Pc13 were pre-incubated 1 h with 100 μM pepstatin A, and immediately after irradiation, cell lysates were submitted to Western blot. Non-treated cells (−) were used as control. Results form one representative experiment are shown (left panels). Densitometric analyses correspond to mean ± S.E.M. of three different experiments (right panels). $^{*}p < 0.01$, $^{**}p < 0.005$, significantly different from control (absence of Pc13); $^{\#}p < 0.05$, significantly different from Pc13-treated cells (without pepstatin A). (C) KB cells incubated in the absence or presence of 5 μM of Pc13 for 24 h were stained with MitoTracker Green and kept in the dark or exposed to a 2.8 J cm$^{-2}$ light dose and then incubated for an additional 1 h. After fixation, cells were incubated with anti-Bax antibody and revealed with a secondary antibody conjugated with Alexa Fluor 568. Nuclei were stained with Hoescht. Magnification 600×, scale bar 10 μm.

membranes (Fig. 2D). In order to determine whether cathepsin D is involved in the phototoxic action of Pc13, we also studied the effect of an aspartic protease inhibitor, pepstatin A, on KB cell proliferation (Ollinger, 2000; Johansson et al., 2003). As shown in Fig. 3A, the growth inhibitory activity induced by Pc13 was partially reverted in the presence of 40–60 μM concentrations of pepstatin A, suggesting that cathepsin D would be in part mediating Pc13 phototoxicity. In addition to cathepsin D, lysosomal permeabilization makes possible the release of other proteases to the cytosol (Roberg et al., 1999; Kågedal et al., 2001). It has been reported that different lysosomal enzymes seem to play a role in the regulation of the apoptotic cell death, being the response dependent on the type of cell and stimulus (Guicciardi et al., 2004; Tardy et al., 2006; Boya and Kroemer, 2008; Johansson et al., 2010; Repnik et al., 2012). Among the wide variety of hydrolytic enzymes that can be released from lysosomes, the well-characterized cathepsins comprise not only the aspartic protease cathepsin D, but also cysteine (B, C, H, L, S) and serine (A, G) proteases (Turk et al., 2002; Turk et al., 2012). The possible contribution of other cathepsins to Pc13-induced cytotoxic action was examined by using leupeptin, a cysteine and serine protease inhibitor (Øverbye et al., 2011). When Pc13-loaded cells were incubated with 25 μM leupeptin, a significant increase of cell viability was observed after photodynamic treatment, suggesting that, in addition to cathepsin D, other proteolytic enzymes are involved in the cell death process triggered by Pc13 (Fig. 3B). A higher percentage of cell proliferation (corresponding to the effect of each individual inhibitor on cell growth) was also obtained when cells were treated in the presence of both pepstatin A and leupeptin (Fig. 3B).

### 3.3. *Pc13 modifies the balance of Bcl-2 family proteins and induces the release of cytochrome C*

We have formerly demonstrated that Pc13 induces an apoptotic response mediated by activation of caspase-3 (Marino et al.,

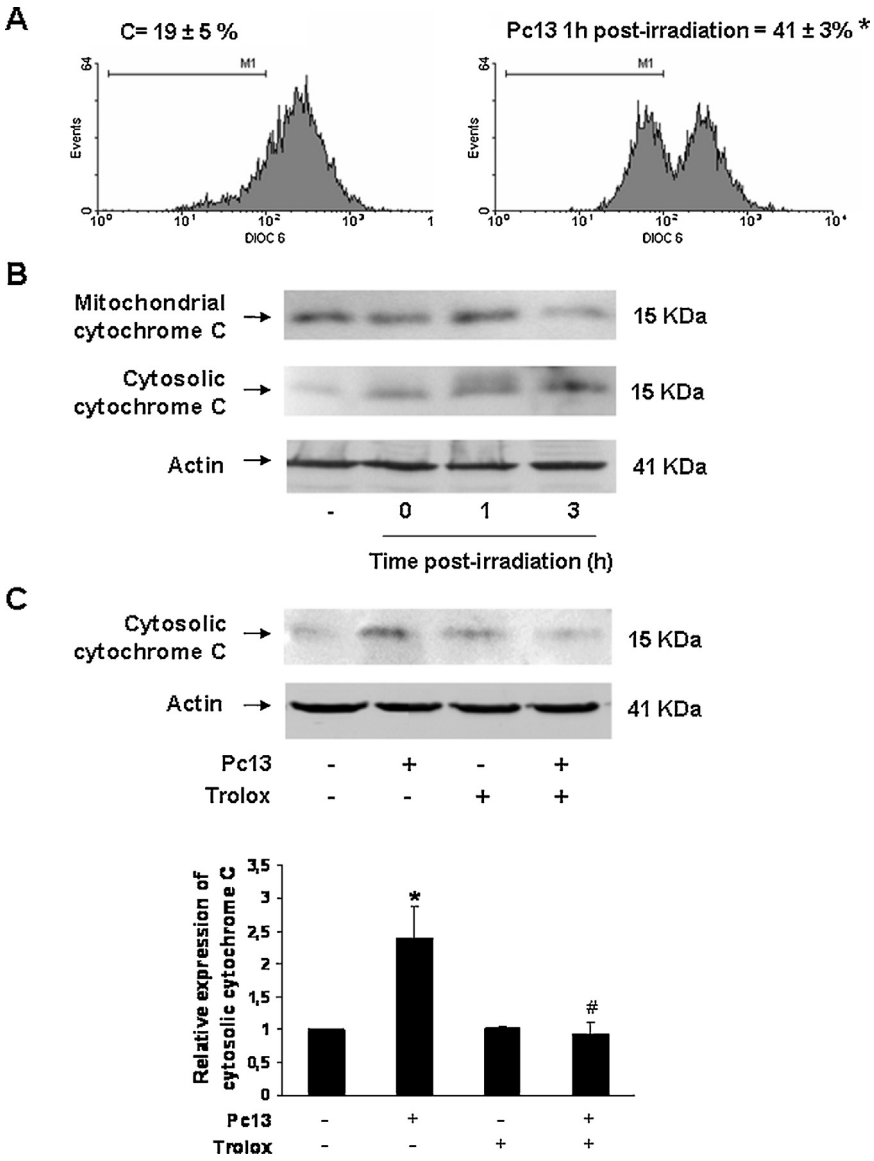


**Fig. 5.** Mitochondrial membrane permeabilization induced by Pc13. (A) After irradiation of KB cells pre-loaded with or without 5 μM Pc13, cells were incubated 1 h and then stained with 40 nM $DiOC_6(3)$ for 30 min. The decrease in $\Delta\Psi_m$ was determined by FACS analysis. $^*p < 0.005$, significantly different from control (absence of Pc13). (B) Representative Western blot assay of cytochrome C detected in mitochondrial and cytosolic fractions obtained after irradiation of KB cells exposed to 5 μM Pc13. Non-treated cells (−) were used as control. (C) Pc13-loaded cells were incubated in the absence or presence of 5 mM trolox and 3 h after irradiation cytosolic fractions were submitted to Western blot. Densitometric analyses, expressed as the relationship of cytosolic cytochrome C from Pc13-treated cells with respect to non-treated cells, correspond to mean ± S.E.M. of three different experiments. $^*p < 0.001$, significantly different from control (absence of Pc13); $^\#p < 0.005$ significantly different from Pc13-treated cells (without trolox).

2010). In order to elucidate the molecular pathways associated with apoptosis, we herein evaluated if the phototoxic effect of Pc13 induced a change in the expression of some Bcl-2 family proteins. In particular, it has been reported that cathepsin D and other lysosomal proteases can be involved in Bid activation and the formation of tBid, a truncated form engaged in the permeabilization of the mitochondrial outer membrane (Stoka et al., 2001; Reiners et al., 2002; Droga-Mazovec et al., 2008; Appelqvist et al., 2012). Based on these findings, we decided to examine the expression levels of full-length Bid protein at different times after irradiation. In addition, we also determined the levels of the pro-apoptotic Bax protein and the anti-apoptotic proteins Bcl-2 and Bcl-$X_L$. Results obtained by Western blot assays showed that the amount of Bax remained unchanged after irradiation of KB cells pre-loaded with Pc13, while a significant decrease of full-length Bid was observed immediately post-irradiation (Fig. 4A). Furthermore, a reduction of the expression levels of the anti-apoptotic proteins Bcl-$X_L$ and Bcl-2 was observed 1 and 3 h after light exposure of Pc13-treated cell (Fig. 4A). We further showed that full-length Bid cleavage was inhibited in the presence of pepstatin A, suggesting that cathepsin D, at least in part, contributes to Bid activation (Fig. 4B). The involvement of lysosomal proteases-mediated Bid cleavage to apoptosis has also been reported for other lysosome-targeted photosensitizers, such as the N-aspartyl chlorine e6 (Reiners et al., 2002; Wan et al., 2008) and the silicon phthalocyanine photosensitizer Pc181 (Chiu et al., 2010). Although these reports did emphasize the role of Bid as a mediator of a PDT-triggered apoptotic response, the lysosomal proteases responsible for proteolytic Bid activation were not identified.

Taking into account that different studies have reported a translocation of Bax from the cytosol to the mitochondria during apoptosis (Wolter et al., 1997; Nechushtan et al., 2001; Hou and Hsu, 2005), we inquired whether Pc13 could induce Bax movement to mitochondria. Bax distribution was evaluated by confocal microscopy after incubating KB cells for 24 h with Pc13 in the dark and staining first with MitoTracker Green and then with an anti-Bax antibody. As shown in Fig. 4C (upper panel), a cytosolic punctuate staining of Bax was detected, but Bax did not show a mitochondrial localization in the dark since no overlapping of the red fluorescence

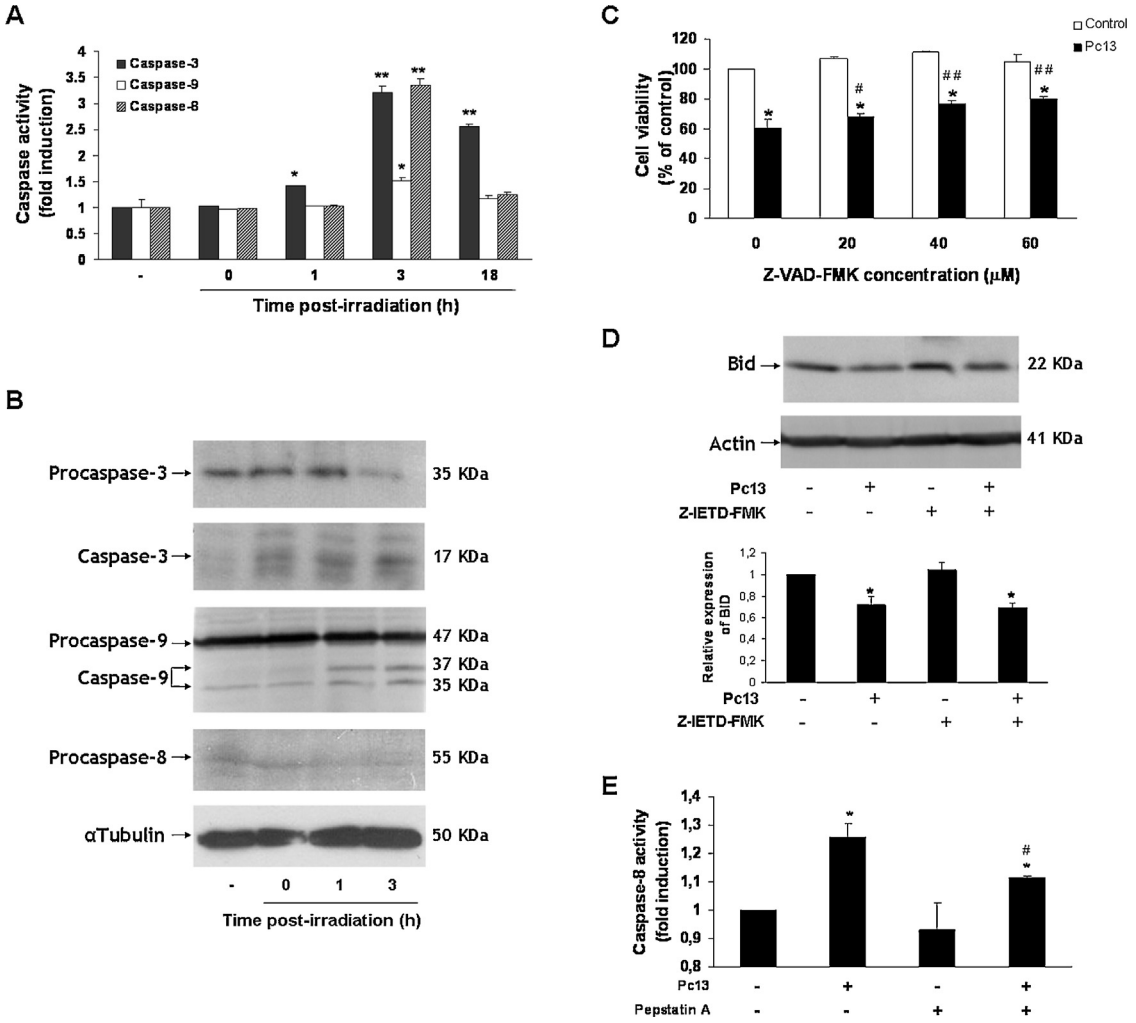


**Fig. 6.** Involvement of caspases in Pc13-induced phototoxic effect. KB cells loaded with or without 5 μM of Pc13 were irradiated with a light dose of 2.8 J $cm^{-2}$ and incubated for different time-periods. (A) Caspase activity was determined as indicated in Section 2. Enzymatic activity is expressed as fold induction with respect to non-treated cells (−) and represents the mean values ± S.E.M. of three different experiments. Statistical significance in comparison with the corresponding control is indicated by $^{*}p < 0.01$ or $^{**}p < 0.0001$. (B) Western blot assays of procaspases or active fragments of caspase-3, -8 and -9. Results from one representative experiment are shown. (C) Pc13-treated cells were pre-incubated 1 h before irradiation with different concentrations of Z-VAD-FMK. Cell growth was determined by the hexosaminidase method. $^{*}p < 0.0001$, significantly different from control (absence of Pc13); $^{\#}p < 0.05$, $^{\#\#}p < 0.0001$ significantly different from cells treated with Pc13 in the absence of Z-VAD-FMK. (D) Pc13-treated cells were pre-incubated 1 h with 20 μM Z-IETD-FMK, and immediately after irradiation, cell lysates were submitted to Western blot with anti-Bid antibody. Densitometric analyses correspond to mean ± S.E.M. of three different experiments. $^{*}p < 0.001$, significantly different from the corresponding controls (absence of Pc13). (E) After incubating Pc13-loaded cells with 100 μM pepstatin A, cells were irradiated and caspase-8 activity was determined 3 h post-irradiation as indicated in Section 2. $^{*}p < 0.05$, $^{**}p < 0.005$, significantly different from control (absence of Pc13); $^{\#}p < 0.05$, significantly different from cells treated with Pc13 in the absence of pepstatin A.

from Bax and the green signal from mitochondrias was observed. However, when KB cells treated with Pc13 were irradiated and then incubated for an additional 1 h, yellow vesicles corresponding to the overlay of Bax and the mitochondrial probe were visualized, indicating Bax mitochondrial translocation after irradiation (Fig. 4C, lower panel).

The activation of the mitochondrial pathway was also explored by determining the loss of the mitochondrial inner transmembrane potential ($\Delta\Psi_m$) by flow cytometry. As shown in Fig. 5A, a significant decrease of $\Delta\Psi_m$ was evident 1 h after the photodynamic action of Pc13, being the percentage of cells with reduced $DiOC_6(3)$ incorporation of $41 \pm 3\%$ versus $19 \pm 5\%$ corresponding to control cells (non-treated cells). In addition, although cytosolic cytochrome C was found at time 0 post-irradiation, maximal levels were obtained 3 h after irradiation, concurrently with a decrease of the cytochrome C amount detected in the mitochondrial fraction (Fig. 5B). We further demonstrated that the release of cytochrome C into the cytosol was completely inhibited in the presence of trolox (Fig. 5C), suggesting that ROS are upstream mediators of mitochondrial membrane permeabilization.

### 3.4. Activation of caspase-dependent pathways mediates the apoptosis induced by Pc13

The interaction of death receptors, such as Fas, tumor necrosis factor receptor or DR5, with their corresponding ligands in the cell surface promotes the recruitment of the adaptor molecule FADD (Fas-associated death domain protein) and procaspase-8, forming the death-inducing signaling complex (DISC). Activation of procaspase-8 at the DISC triggers the death receptor or extrinsic pathway (Hengartner, 2000; Kaufmann and Hengartner, 2001; Chaudhari et al., 2006). When the mitochondrial pathway is mediating an apoptotic cell death, the release of cytochrome C from the mitochondria leads to the activation of caspase-9 and the formation of the apoptosome, a cytosolic death signaling complex (Kaufmann and Hengartner, 2001; Green and Reed, 1998; Thornberry and Lazebnik, 1998; Grutter, 2000). In order to evaluate the dependence of caspase-8 and caspase-9 activation on Pc13-mediated apoptosis, we measured the proteolytic activity of both initiator caspases together with the activity of the executioner caspase-3. As shown in Fig. 6A, caspase-3 and -8 activation reached a peak (3–3.5-fold increase) after 3 h of light exposure, and the same incubation time was required to detect a slight but significant increment in caspase-9 activity (1.5-fold). Caspases activation was also confirmed by Western blot assays. Thus, a significant decrease of full length caspase-3 was evident after 3 h of irradiation of Pc13-loaded cells, although the active 17-kDa fragment was early detected at time 0 post-irradiation when an antibody against the cleaved caspase-3 was employed (Fig. 6B). In addition, lower levels of procaspase 8 (55 kDa) were detected 1 h post-irradiation, while cleaved fragments of 35/37 kDa derived from caspase-9 (47 kDa) were evident 1 and 3 h after light treatment (Fig. 6B).

The involvement of caspases in the phototoxic action of Pc13 was next examined by determining cell viability in the presence of the pan inhibitor Z-VAD-FMK. As shown in Fig. 6C, the growth inhibitory activity induced by Pc13 was partially reverted in the presence of increasing concentrations of Z-VAD-FMK, indicating that caspases would be to some extent mediating Pc13 phototoxicity.

Taking into account that Pc13 is mainly localized in lysosomes, activation of caspase-8 mediated by death receptor pathway would be unlikely. In fact, no change in the expression levels of Fas/Fas-L and TRAIL/DR5 were detected after Western blot assays of lysates from irradiated Pc13-loaded cells (data not shown). Nevertheless, since it has been reported that activation of caspase-8 could be responsible for Bid truncation (Li et al., 1998; Luo et al., 1998), we further examined if caspase-8 could contribute to Bid processing at time 0 post-irradiation. In this respect, although caspase-8 activation was detected 1 h after irradiation (Fig. 6B), it is possible to assume that a low level of caspase-8 activation (under detection limits) could be enough to produce an early Bid cleavage. As shown in Fig. 6D, caspase-8 inhibitor Z-IETD-FMK did not modify Bid expression levels, indicating that caspase-8 did not participate in Bid truncation.

Since it has been reported that cathepsin D directly activates caspase-8 in neutrophil apoptosis (Conus et al., 2008), we decided to study the effect of a cathepsin D inhibitor on caspase-8 proteolysis. When KB cells treated with Pc13 were pre-incubated with pepstatin A, irradiated with a light dose of $1.4\,J\,cm^{-2}$ and then incubated for another 3 h, the increase of caspase-8 activity was significantly inhibited, indicating that cathepsin D contributes, at least partially, to caspase-8 activation (Fig. 6E). Although we did not evaluate a direct effect of cathepsin D on caspase-8, this result indicated that the lysosomal protease would be acting as an upstream modulator of caspase-8 activation.

## 4. Conclusions

In this study, we explored the molecular mechanisms responsible for the apoptotic response induced by the lysosome-targeted cationic photosensitizer Pc13 in human nasopharynx KB carcinoma cells (Fig. 7). Immediately after irradiation of KB cells pre-loaded with Pc13, ROS formation triggers the sequence of events which finally lead to cell death. Thus, the generation of ROS in the primary site of Pc13 accumulation early affects lysosomal membrane permeabilization, leading to the release of lysosomal proteases to cytosol. Subsequent cathepsin D-mediated Bid processing together with the decrease expression of anti-apoptotic proteins and the translocation of Bax from cytosol to mitochondria contribute to the activation of the mitochondrial pathway of apoptosis.

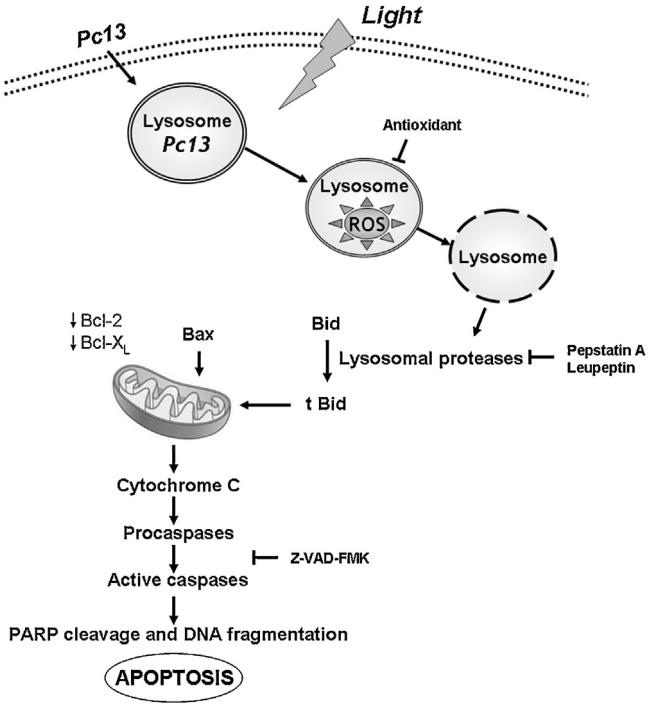


**Fig. 7.** Proposed model of Pc13-induced apoptosis in KB cells. The formation of ROS in the primary site of Pc13 accumulation leads to lysosomal membrane permeabilization followed by the release of lysosomal proteases, alteration of Bcl-2 family proteins and activation of a caspase-dependent pathway downstream mitochondrial injury.

Mitochondrial membrane depolarization and release of cytochrome C highlight the dysfunction of the mitochondria. Both caspase-dependent and independent mechanisms of apoptotic cell death have been described for other photosensitizers localized mainly in lysosomes (Reiners et al., 2002; Vittar et al., 2010). Results herein obtained show that a caspase-dependent pathway activated downstream mitochondrial injury also contributes to Pc13-induced apoptosis, although the involvement of caspase-independent factors in the phototoxic effect of Pc13 cannot be discarded.

## Acknowledgments

This work was supported by grants from Consejo Nacional de Investigaciones Científicas y Técnicas (CONICET, PIP 1261 and PIP 0104), Universidad de Buenos Aires (UBACYT 20020100100081), Argentina.

## References

Allen CM, Langlois R, Sharman WM, La Madeleine C, Van Lier JE. Photodynamic properties of amphiphilic derivatives of aluminum tetrasulfophthalocyanine. Photochem Photobiol 2002;76:208–16.
Allison RR, Bagnato VS, Sibata CH. Future of oncologic photodynamic therapy. Future Oncol 2010;6:929–40.
Appelqvist H, Johansson AC, Linderoth E, Johansson U, Antonsson B, Steinfeld R, et al. Lysosome-mediated apoptosis is associated with cathepsin D-specific processing of Bid at Phe24, Trp48, and Phe183. Ann Clin Lab Sci 2012;42:231–42.
Boya P, Gonzalez-Polo RA, Poncet D, Andreau K, Vieira HL, Roumier T, et al. Mitochondrial membrane permeabilization is a critical step of lysosome-initiated apoptosis induced by hydroxychloroquine. Oncogene 2003;22:3927–36.
Boya P, Kroemer G. Lysosomal membrane permeabilization in cell death. Oncogene 2008;27:6434–51.
Boyle RW, Paquette B, van Lier JE. Biological activities of phthalocyanines XIV. Effect of hydrophobic phthalimidomethyl groups on the in vivo phototoxicity and mechanism of photodynamic action of sulphonated aluminium phthalocyanines. Br J Cancer 1992;65:813–7.
Calzavara-Pinton PG, Venturini M, Sala R. Photodynamic therapy: update 2006 Part 1: photochemistry and photobiology. J Eur Acad Dermatol Venereol 2007;21:293–302.
Chaudhari BR, Murphy RF, Agrawal DK:. Following the TRAIL to apoptosis. Immunol Res 2006;35:249–62.
Chiu SM, Xue LY, Lam M, Rodriguez ME, Zhang P, Kenney ME, et al. A requirement for bid for induction of apoptosis by photodynamic therapy with a lysosome- but not a mitochondrion-targeted photosensitizer. Photochem Photobiol 2010;86:1161–73.
Chwieralski CE, Welte T, Bühling F. Cathepsin-regulated apoptosis. Apoptosis 2006;11:143–9.
Colussi VC, Feyes DK, Mulvihill JW, Li YS, Kenney ME, Elmets CA, et al. Phthalocyanine 4 (Pc 4) photodynamic therapy of human OVCAR-3 tumor xenografts. Photochem Photobiol 1999;69:236–41.
Conus S, Perozzo R, Reinheckel T, Peters C, Scapozza L, Yousefi S, et al. Caspase-8 is activated by cathepsin D initiating neutrophil apoptosis during the resolution of inflammation. J Exp Med 2008;205:685–98.
Droga-Mazovec G, Bojic L, Petelin A, Ivanova S, Romih R, Repnik U, et al. Cysteine cathepsins trigger caspase-dependent cell death through cleavage of bid and antiapoptotic Bcl-2 homologues. J Biol Chem 2008;283:19140–50.
Green DR, Reed JC. Mitochondria and apoptosis. Science 1998;281:1309–12.
Grutter MG. Caspases: key players in programmed cell death. Curr Opin Struct Biol 2000;10:649–55.
Guicciardi ME, Leist M, Gores GJ. Lysosomes in cell death. Oncogene 2004;23:2881–90.
Hasilik A. The early and late processing of lysosomal enzymes: proteolysis and compartmentation. Experientia 1992;48:130–51.
Henderson BW, Dougherty TJ. How does photodynamic therapy work? Photochem Photobiol 1992;55:145–57.
Hengartner MO. The biochemistry of apoptosis. Nature 2000;407:770–6.
Hou Q, Hsu YT. Bax translocates from cytosol to mitochondria in cardiac cells during apoptosis: development of a GFP-Bax-stable H9c2 cell line for apoptosis analysis. Am J Physiol Heart Circ Physiol 2005;289:H477–87.
Johansson AC, Appelqvist H, Nilsson C, Kågedal K, Roberg K, Ollinger K. Regulation of apoptosis-associated lysosomal membrane permeabilization. Apoptosis 2010;15:527–40.
Johansson AC, Steen H, Ollinger K, Roberg K. Cathepsin D mediates cytochrome c release and caspase activation in human fibroblast apoptosis induced by staurosporine. Cell Death Differ 2003;10:1253–9.
Kågedal K, Johansson U, Ollinger K. The lysosomal protease cathepsin D mediates apoptosis induced by oxidative stress. FASEB J 2001;15:1592–4.
Kaufmann SH, Hengartner MO. Programmed cell death: alive and well in the new millennium. Trends Cell Biol 2001;11:526–34.
Landegren U. Measurement of cell numbers by means of the endogenous enzyme hexosaminidase. Applications to detection of lymphokines and cell surface antigens. J Immunol Methods 1984;67:379–88.
Lawless MW, Mankan AK, Gray SG, Norris S. Endoplasmic reticulum stress—a double edged sword for Z alpha-1 antitrypsin deficiency hepatoxicity. Int J Biochem Cell Biol 2008;40:1403–14.
Li H, Jensen TJ, Fronczek FR, Vicente MG. Syntheses and properties of a series of cationic water-soluble phthalocyanines. J Med Chem 2008;51:502–11.
Li H, Zhu H, Xu CJ, Yuan J. Cleavage of BID by caspase 8 mediates the mitochondrial damage in the Fas pathway of apoptosis. Cell 1998;94:491–501.
Liu L, Zhang Z, Xing D. Cell death via mitochondrial apoptotic pathway due to activation of Bax by lysosomal photodamage. Free Radic Biol Med 2011;51:53–68.
Luo X, Budihardjo I, Zou H, Slaughter C, Wang X. Bid, a Bcl2 interacting protein, mediates cytochrome c release from mitochondria in response to activation of cell surface death receptors. Cell 1998;94:481–90.
Margaron P, Grégoire MJ, Scasnár V, Ali H, van Lier JE. Structure-photodynamic activity relationships of a series of 4-substituted zinc phthalocyanines. Photochem Photobiol 1996;63:217–23.
Marino J, García Vior MC, Dicelio LE, Roguin LP, Awruch J. Photodynamic effects of isosteric water-soluble phthalocyanines on human nasopharynx KB carcinoma cells. Eur J Med Chem 2010;45:4129–39.
Miller JD, Baron ED, Scull H, Hsia A, Berlin JC, McCormick T, et al. Photodynamic therapy with the phthalocyanine photosensitizer Pc 4: the case experience with preclinical mechanistic and early clinical-translational studies. Toxicol Appl Pharmacol 2007;224:290–9.
Nechushtan A, Smith CL, Lamensdorf I, Yoon SH, Youle RJ. Bax and Bak coalesce into novel mitochondria-associated clusters during apoptosis. J Cell Biol 2001;153:1265–76.
Oleinick NL, Morris RL, Belichenko I. The role of apoptosis in response to photodynamic therapy: what, where, why, and how. Photochem Photobiol Sci 2002;1:1–21.
Ollinger K. Inhibition of cathepsin D prevents free-radical-induced apoptosis in rat cardiomyocytes. Arch Biochem Biophys 2000;373:346–51.
Øverbye A, Sætre F, Hagen LK, Johansen HT, Seglen PO. Autophagic activity measured in whole rat hepatocytes as the accumulation of a novel BHMT fragment (p10), generated in amphisomes by the asparaginyl proteinase, legumain. Autophagy 2011;7:1011–27.
Paquette B, Boyle RW, Ali H, MacLennan AH, Truscott TG, van Lier JE. Sulfonated phthalimidomethyl aluminum phthalocyanine: the effect of hydrophobic substituents on the in vitro phototoxicity of phthalocyanines. Photochem Photobiol 1991;53:323–7.
Reiners JJ Jr, Caruso JA, Mathieu P, Chelladurai B, Yin XM, Kessel D. Release of cytochrome c and activation of pro-caspase-9 following lysosomal photodamage involves Bid cleavage. Cell Death Differ 2002;9:934–44.
Repnik U, Stoka V, Turk V, Turk B. Lysosomes and lysosomal cathepsins in cell death. Biochim Biophys Acta 2012;1824:22–33.
Roberg K, Johansson U, Ollinger K. Lysosomal release of cathepsin D precedes relocation of cytochrome c and loss of mitochondrial transmembrane potential during apoptosis induced by oxidative stress. Free Radic Biol Med 1999;27:1228–37.
Sharman WM, Allen CM, van Lier JE. Photodynamic therapeutics: basic principles and clinical applications. Drug Discov Today 1999;11:507–17.
Stoka V, Turk B, Schendel SL, Kim TH, Cirman T, Snipas SJ, et al. Lysosomal protease pathways to apoptosis. Cleavage of bid, not pro-caspases, is the most likely route. J Biol Chem 2001;276:3149–57.
Taquet JP, Frochot C, Manneville V, Barberi-Heyob M. Phthalocyanines covalently bound to biomolecules for a targeted photodynamic therapy. Curr Med Chem 2007;14:1673–87.
Tardy C, Codogno P, Autefage H, Levade T, Andrieu-Abadie N. Lysosomes and lysosomal proteins in cancer cell death (new players of an old struggle). Biochim Biophys Acta 2006;1765:101–25.
Thornberry NA, Lazebnik Y. Caspases: enemies within. Science 1998;281:1312–6.
Turk B, Stoka V, Rozman-Pungercar J, Cirman T, Droga-Mazovec G, Oresić K, et al. Apoptotic pathways: involvement of lysosomal proteases. Biol Chem 2002;383:1035–44.
Turk V, Stoka V, Vasiljeva O, Renko M, Sun T, Turk B, et al. Cysteine cathepsins: from structure, function and regulation to new frontiers. Biochim Biophys Acta 2012;1824:68–88.
Vittar NB, Awruch J, Azizuddin K, Rivarola V. Caspase-independent apoptosis, in human MCF-7c3 breast cancer cells, following photodynamic therapy, with a novel water-soluble phthalocyanine. Int J Biochem Cell Biol 2010;42:1123–31.
Wan Q, Liu L, Xing D, Chen Q. Bid is required in NPe6-PDT-induced apoptosis. Photochem Photobiol 2008;84:250–7.
Welinder C, Ekblad L. Coomassie staining as loading control in Western blot analysis. J Proteome Res 2011;10:1416–9.
Wolter KG, Hsu YT, Smith CL, Nechushtan A, Xi XG, Youle RJ. Movement of Bax from the cytosol to mitochondria during apoptosis. J Cell Biol 1997;139:1281–92.